# Double Diffractive Cross-Section Measurement in the Forward Region at the LHC

G. Antchev *et al.**
(TOTEM Collaboration)

(Received 29 August 2013; revised manuscript received 1 October 2013; published 26 December 2013)

The first double diffractive cross-section measurement in the very forward region has been carried out by the TOTEM experiment at the LHC with a center-of-mass energy of $\sqrt{s} = 7$ TeV. By utilizing the very forward TOTEM tracking detectors $T1$ and $T2$, which extend up to $|\eta| = 6.5$, a clean sample of double diffractive pp events was extracted. From these events, we determined the cross section $\sigma_{\mathrm{DD}} = (116 \pm 25)\ \mu$b for events where both diffractive systems have $4.7 < |\eta|_{\mathrm{min}} < 6.5$.

DOI: 10.1103/PhysRevLett.111.262001 PACS numbers: 13.85.Ni

Diffractive scattering represents a unique tool for investigating the dynamics of strong interactions and proton structure. These events are dominated by soft processes which cannot be calculated with perturbative QCD. Various model calculations predict diffractive cross sections that are markedly different at the LHC energies [1–3].

Double diffractive dissociation (DD) is the process in which two colliding hadrons dissociate into clusters of particles, and the interaction is mediated by an object with the quantum numbers of the vacuum. Experimentally, DD events are typically associated with a rapidity gap that is large compared to random multiplicity fluctuations. Rapidity gaps are exponentially suppressed in nondiffractive (ND) events [4]; however, when a detector is not able to detect particles with the transverse momentum ($p_T$) of a few hundred MeV, the identification of double diffractive events by means of rapidity gaps becomes very challenging. The excellent $p_T$ acceptance of the TOTEM detectors makes the experiment favorable for the measurement. Previous measurements of the DD cross section are described in Refs. [5,6].

The TOTEM experiment [7] is a dedicated experiment to study diffraction, total cross section, and elastic scattering at the LHC. It has three subdetectors placed symmetrically on both sides of the interaction point: Roman pot detectors (RPs) to identify leading protons and $T1$ and $T2$ telescopes to detect charged particles in the forward region. The most important detectors for this measurement are the $T2$ and $T1$ telescopes. $T2$ consists of gas electron multipliers that detect charged particles with $p_T > 40$ MeV/$c$ at pseudorapidities of $5.3 < |\eta| < 6.5$ [8]. The $T1$ telescope consists of cathode strip chambers that measure charged particles with $p_T > 100$ MeV/$c$ at $3.1 < |\eta| < 4.7$.

In this novel measurement, the double diffractive cross section was determined in the forward region. The method is as model independent as possible. The DD events were selected by vetoing $T1$ tracks and requiring tracks in $T2$, hence selecting events that have two diffractive systems with $4.7 < |\eta|_{\mathrm{min}} < 6.5$, where $\eta_{\mathrm{min}}$ is the minimum pseudorapidity of all primary particles produced in the diffractive system. Although these events are only about 3% of the total $\sigma_{\mathrm{DD}}$, they provide a pure selection of DD events and the measurement is an important step towards determining if there is a rich resonance structure in the low mass region [9]. To probe further, the $\eta_{\mathrm{min}}$ range was divided into two subregions on each side, providing four subcategories for the measurement.

The analysis is structured in three steps. In the first step, the raw rate of double diffractive events is estimated: the selected sample is corrected for trigger efficiency, pileup, and $T1$ multiplicity, and the amount of background is determined. In the second step, the visible cross section, i.e., the cross section for events that have at least one particle in both sides of $5.3 < |\eta| < 6.5$ and no particles within $3.1 < |\eta| < 4.7$, is calculated by correcting the raw rate up to the particle level. Because roughly half of neutral only events produce a charged secondary particle [10], the acceptance and efficiency of detecting both charged and neutral particles are considered in the corrections. In the last step, the visible cross section is corrected so that both diffractive systems have $4.7 < |\eta|_{\mathrm{min}} < 6.5$. This $|\eta|_{\mathrm{min}}$ range roughly corresponds to the diffractive mass range of $3.4 < M_{\mathrm{diff}} < 8.0$ GeV.

This measurement uses data collected in October 2011 at $\sqrt{s} = 7$ TeV during a low pileup run with a special $\beta^* = 90$ m optics. The data were collected with the $T2$ minimum bias trigger. The trigger condition was that three out of 10 superpads in the same $r - \phi$ sector fired. A superpad consists of three radial and five azimuthal neighboring pads, and it is sufficient that one out of 15 pads registered a signal for a superpad to be fired.

After the off-line reconstruction of $T2$ and $T1$ tracks [11,12], the DD events were selected by requiring tracks in

*Full author list given at the end of the article.



 

both $T2$ arms and no tracks in either of the $T1$ arms ($2T2 + 0T1$). $T2$ tracks with a $\chi^2$-fit probability smaller than 2% and tracks falling in the overlap region of two $T2$ quarters, i.e., tracks with $80° < \phi < 100°$ or $260° < \phi < 280°$, were removed. The tracks in the overlap region were removed because simulation does not model well their response. In the Letter, this full selection for a visible cross section is named $I_{\text{track}}$. The four subcategories for the visible cross-section measurement were defined by the $T2$ track with minimum $|\eta|$ on each side, $|\eta^{+}_{\text{track}}|_{\text{min}}$ and $|\eta^{-}_{\text{track}}|_{\text{min}}$. The subcategory $D11_{\text{track}}$ includes the events with $5.3 < |\eta^{\pm}_{\text{track}}|_{\text{min}} < 5.9$, $D22_{\text{track}}$ the events with $5.9 < |\eta^{\pm}_{\text{track}}|_{\text{min}} < 6.5$, $D12_{\text{track}}$ the events with $5.3 < |\eta^{+}_{\text{track}}|_{\text{min}} < 5.9$ and $5.9 < |\eta^{-}_{\text{track}}|_{\text{min}} < 6.5$, and $D21_{\text{track}}$ the events with $5.9 < |\eta^{+}_{\text{track}}|_{\text{min}} < 6.5$ and $5.3 < |\eta^{-}_{\text{track}}|_{\text{min}} < 5.9$.

Two additional samples were extracted for background estimation. A control sample for single diffractive (SD) events has at least one track in either of the $T2$ arms and no tracks in the opposite side $T2$ arm nor in $T1$ ($1T2 + 0T1$). A control sample for ND events has tracks in all arms of $T2$ and $T1$ detectors ($2T2 + 2T1$). Four additional exclusive data samples were defined for testing the background model validity: tracks in both arms of $T2$ and exactly in one arm of $T1$ ($2T2 + 1T1$), tracks in either of $T2$ arms and in both $T1$ arms ($1T2 + 2T1$), tracks in $T2$ and $T1$ in one side of the interaction point ($1T2 + 1T1$ same side), and tracks in $T2$ and $T1$ in the opposite side of the interaction point ($1T2 + 1T1$ opposite side). Each sample corresponds to one signature type $j$.

The number of selected data events was corrected for trigger efficiency and pileup. The trigger efficiency correction $c_t$ was calculated from a zero-bias triggered sample in the bins of number of tracks. It is described in detail in Ref. [13]. The pileup correction was calculated using the formula

$$c^{j}_{\text{pu}} = \frac{1}{1 - \frac{2p_{\text{pu}}}{1+p_{\text{pu}}} + \frac{2p_{\text{pu}}}{1+p_{\text{pu}}} p^{j}}, \tag{1}$$

where $j$ is the signature type, $p_{\text{pu}} = (1.5 \pm 0.4)\%$ is the pileup correction factor for inelastic events [13], and $p^j$ is the correction for signature type changes due to pileup. The correction $p^j$ was determined by creating a Monte Carlo (MC) study of pileup. A pool of signature types was created by weighting each type with their probability in the data. Then a pair was randomly selected, and their signatures were combined. After repeating the selection and combination, the correction was calculated as $p^j = N^j_{\text{combined}}/N^j_{\text{original}}$. $N^j_{\text{combined}}$ is the number of selected combinations that have the combined signature of $j$. The uncertainty in $p^j$ was determined by taking the event type weights from PYTHIA 8.108 default tune [14] and recalculating $p^j$. The values of uncertainties of $p^j$ are between 10% and 40%, depending on signature type $j$. The values for overall pileup correction factors $c^j_{\text{pu}}$ are between 0.99 and 1.03. The signature type $2T2 + 2T1$ has the correction factor of 0.99; all other signature types have correction factors that are greater than 1. Finally, the corrected number of data events were calculated with the formula $N^j = c_t c^j_{\text{pu}} N^j_{\text{raw}}$.

The simulated $T1$ track multiplicity distribution predicts a lower number of zero-track events than what was observed in the data. The number of $T1$ tracks in the simulation was corrected to match with the data by randomly selecting 10% (2%) of one-(two-)track events and changing them to zero-track events.

Three kinds of background were considered for the analysis: ND, SD and central diffraction (CD). ND and SD background estimation methods were developed to minimize the model dependence, and the values of estimates were calculated iteratively. Since the CD background is significantly smaller than the ND and SD ones, its estimate ($N_{\text{CD}}$) was taken from simulation, using the acceptance and $\sigma_{\text{CD}} = 1.3$ mb from PHOJET 1.12 [15].

The number of ND events in the ND dominated control sample, $2T2 + 2T1$, has been determined as

$$N^{2T2+2T1}_{\text{ND}} = N^{2T2+2T1}_{\text{data}} - N^{2T2+2T1}_{\text{DD}} - N^{2T2+2T1}_{\text{SD}} - N^{2T2+2T1}_{\text{CD}}, \tag{2}$$

where $N^{2T2+2T1}_{\text{DD}}$ and $N^{2T2+2T1}_{\text{SD}}$ were taken from MC simulations for the first iteration. PYTHIA was used as the default generator throughout the analysis. The ratio $R^j_{\text{ND}}$ of ND events expected in the sample $j$ and in the control sample, was calculated from MC simulations as

$$R^j_{\text{ND}} = \frac{N^j_{\text{ND,MC}}}{N^{2T2+2T1}_{\text{ND,MC}}}. \tag{3}$$

The number of ND events within the signal sample was estimated as

$$N^j_{\text{ND}} = R^j_{\text{ND}} C^j N^{2T2+2T1}_{\text{ND}}, \tag{4}$$

where $C^j$ is the normalization factor deduced from the relative mismatch between the data and the total PYTHIA prediction in the signal sample,

$$C^j = \frac{N^j_{\text{data}}}{N^j_{\text{MC}}} \frac{N^{2T2+2T1}_{\text{MC}}}{N^{2T2+2T1}_{\text{data}}}. \tag{5}$$

The SD background estimation starts from the calculation of the number of SD events in the SD dominated control sample, $1T2 + 0T1$, by subtracting the number of other kinds of events from the number of data events,

$$N^{1T2+0T1}_{\text{SD}} = N^{1T2+0T1}_{\text{data}} - N^{1T2+0T1}_{\text{DD}} - N^{1T2+0T1}_{\text{ND}} - N^{1T2+0T1}_{\text{CD}}, \tag{6}$$

where $N^{1T2+0T1}_{\text{ND}}$ was calculated with the ND estimation method and $N^{1T2+0T1}_{\text{DD}}$ was taken from PYTHIA for the first iteration. To scale the number of SD events to the signal

TABLE I. Estimated numbers of ND, SD, CD, and DD events in the ND and SD background control samples. The numbers correspond to the full selection $I_{\text{track}}$.

| | ND control sample $2T2 + 2T1$ | SD control sample $1T2 + 0T1$ |
|---|---|---|
| ND | 1 178 737 ± 19 368 | 659 ± 65 |
| SD | 74 860 ± 6954 | 60 597 ± 12 392 |
| CD | 2413 ± 1207 | 2685 ± 1343 |
| DD | 54 563 ± 19 368 | 15 858 ± 1123 |
| Total | 1 310 573 ± 20 614 | 79 798 ± 12 465 |
| Data | 1 310 573 | 79 798 |

region, the ratio $R^j_{\text{SD}}$ was calculated from data. The SD dominated data events that were used in the calculation of the ratio have exactly one leading proton seen by the RPs, in addition to the sample selections based on $T2$ and $T1$ tracks. By using the ratio

$$R^j_{\text{SD}} = \frac{N^{j+1\text{proton}}_{\text{data}}}{N^{1T2+0T1+1\text{proton}}_{\text{data}}}, \tag{7}$$

the expected number of background SD events was calculated as

$$N^j_{\text{SD}} = R^j_{\text{SD}} N^{1T2+0T1}_{\text{SD}}. \tag{8}$$

The first estimate of $\sigma_{\text{DD}}$ was calculated with the ND, SD, and CD background estimates described above. The background estimations were repeated with redefined values of $N^{2T2+2T1}_{\text{DD}}$, $N^{2T2+2T1}_{\text{SD}}$, $N^{1T2+0T1}_{\text{DD}}$, and $N^{1T2+0T1}_{\text{ND}}$: the numbers of DD events were scaled with the ratio of $\sigma^{\text{measured}}_{\text{DD}}/\sigma^{\text{MC}}_{\text{DD}}$, and the numbers of SD and ND events were calculated using their estimation methods. Next, the three steps were repeated until $N^{2T2+0T1}_{\text{ND}}$ and $N^{2T2+0T1}_{\text{SD}}$ converged. The iteration converged to the $2 \times 10^{-5}$ level within three steps. The final numbers of estimates in the $I_{\text{track}}$ control samples are shown in Table I, and the estimated numbers of background events in the signal sample are shown in Table II.

The reliability of the background estimates was examined in the validation samples. In these samples, the total estimated number of events is consistent with the number of data events within the uncertainty of the estimate; see Fig. 1. The uncertainty in the SD estimate was determined

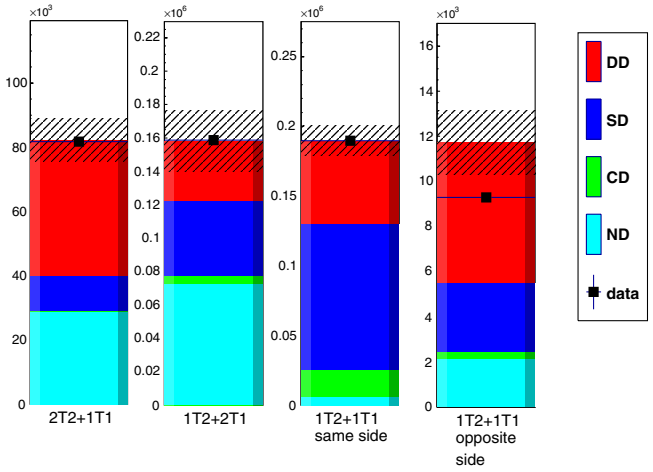


FIG. 1 (color online). Validation of background estimates for the full selection $I_{\text{track}}$. Each plot shows the corrected number of events in data (black squares) and the combined estimate with background uncertainties. The combined estimate is the sum of all components, from bottom to top: the ND estimate (cyan), CD estimate (green), SD estimate (blue), and DD estimate (red).

with an alternative control sample: $1T2 + 1T1$ same side. To determine the uncertainty in the ND estimate, the ratio $R^j_{\text{ND}}$ was calculated from PHOJET and $N^j_{\text{ND}}$ estimated with it. A conservative uncertainty of 50% was assigned for the CD estimate.

The visible DD cross section was calculated using the formula

$$\sigma_{\text{DD}} = \frac{E(N^{2T2+0T1}_{\text{data}} - N^{2T2+0T1}_{\text{bckg}})}{\mathcal{L}}, \tag{9}$$

where $E$ is the experimental correction, $\mathcal{L} = (40.1 \pm 1.6)\ \mu b^{-1}$ is the integrated luminosity, and $N^{2T2+0T1}_{\text{bckg}}$ and $N^{2T2+0T1}_{\text{data}}$ are the total expected background and number of data events from Table II. The experimental correction $E = 0.90 \pm 0.10$ for the $I_{\text{track}}$ selection. The correction $E$ includes the acceptance, the tracking, and reconstruction efficiencies of the $T2$ detector (1.19 for the $I_{\text{track}}$ selection on either side of the IP), the correction of events with only neutral particles within the detector acceptance (1.10), bin migration (0.95), and veto efficiency (0.77). The correction $E$ was estimated using PYTHIA, and the largest

TABLE II. Expected number of background events and observed number of data events passing the signal event selection $2T2 + 0T1$.

| | $I_{\text{track}}$ | $D11_{\text{track}}$ | $D22_{\text{track}}$ | $D12_{\text{track}}$ | $D21_{\text{track}}$ |
|---|---|---|---|---|---|
| ND | 829 ± 239 | 672 ± 100 | 28 ± 22 | 115 ± 16 | 109 ± 23 |
| SD | 1588 ± 381 | 895 ± 321 | 80 ± 76 | 303 ± 95 | 291 ± 77 |
| CD | 7 ± 3 | 5 ± 3 | 1 ± 1 | 1 ± 1 | 1 ± 1 |
| Total expected background | 2424 ± 450 | 1572 ± 336 | 109 ± 79 | 419 ± 96 | 400 ± 80 |
| Data | 8214 | 5261 | 375 | 1350 | 1386 |

TABLE III. Double diffractive cross-section measurements ($\mu$b) in the forward region. Both visible and $\eta_{\min}$ corrected cross sections are given. The latter is compared to PYTHIA and PHOJET predictions. PYTHIA estimate for total $\sigma_{\mathrm{DD}} = 8.1$ mb and PHOJET estimate $\sigma_{\mathrm{DD}} = 3.9$ mb.

| | $I_{\mathrm{track}}$ | $D11_{\mathrm{track}}$ | $D22_{\mathrm{track}}$ | $D12_{\mathrm{track}}$ | $D21_{\mathrm{track}}$ |
|---|---|---|---|---|---|
| Visible | $131 \pm 22$ | $58 \pm 14$ | $20 \pm 8$ | $31 \pm 5$ | $34 \pm 5$ |
| | $I$ | $D11$ | $D22$ | $D12$ | $D21$ |
| $\eta_{\min}$ | $116 \pm 25$ | $65 \pm 20$ | $12 \pm 5$ | $26 \pm 5$ | $27 \pm 5$ |
| PYTHIA $\eta_{\min}$ | 159 | 70 | 17 | 36 | 36 |
| PHOJET $\eta_{\min}$ | 101 | 44 | 12 | 23 | 23 |

difference with respect to QGSJET-II-03 [16] and PHOJET was taken as the uncertainty. The $D12_{\mathrm{track}}$, $D21_{\mathrm{track}}$, and $D22_{\mathrm{track}}$ subcategories have an additional correction factor related to the $5.3 < |\eta_{\mathrm{track}}|_{\min} < 5.9$ veto. Monte Carlo simulations underestimate the number of secondary particles [10], and therefore we checked the veto efficiency from data. $2T2 + 2T1$ and $1T2 + 1T1$ same side selections provide samples where a rapidity gap of $5.3 < |\eta_{\mathrm{track}}| < 5.9$ is not expected. We checked the ratio $N_{5.9<|\eta_{\mathrm{track}}|_{\min}<6.5}/N_{\mathrm{total}}$ between data and MC in the $2T2 + 2T1$ and $1T2 + 1T1$ same side samples, and determined the additional correction factor in such a way that the MC ratio is consistent with data. The value of the correction factor is $1.22 \pm 0.03$ ($1.24 \pm 0.03$) for the positive (negative) side, and it is an additional component to $E$ of the $D12_{\mathrm{track}}$, $D21_{\mathrm{track}}$, and $D22_{\mathrm{track}}$ subcategories.

TOTEM measured the visible cross section of $\sigma_{\mathrm{DD}} = (131 \pm 22)$ $\mu$b for events that have at least one particle in both sides of $5.3 < |\eta| < 6.5$ and no particles within $3.1 < |\eta| < 4.7$. The visible cross-section measurements of the subcategories are summarized in Table III.

Diffractive system can still have $\eta_{\min}$ in the uninstrumented region; i.e., on either side of the IP one can write the formula for the number of visible events,

$$N_{\mathrm{visible}} = N_{5.3<|\eta|_{\min}<6.5} + N^{\mathrm{visible}}_{4.7<|\eta|_{\min}<5.3} + N^{\mathrm{visible}}_{|\eta|_{\min}<3.1}. \quad (10)$$

All the events with $5.3 < |\eta|_{\min} < 6.5$ are visible, whereas some of the $4.7 < |\eta|_{\min} < 5.3$ and $|\eta|_{\min} < 3.1$ events are visible by the selection.

To minimize the model dependence, two options were studied for the $\eta_{\min}$ range: $5.3 < |\eta^{\pm}|_{\min} < 6.5$ and $4.7 < |\eta^{\pm}|_{\min} < 6.5$. The first option benefits from the fact that all such events are included in the visible sample, whereas the latter benefits from the fact that a significant share of $4.7 < |\eta^{\pm}|_{\min} < 5.3$ events are visible by the selection. The correction was determined from generator level PYTHIA by calculating the ratios of $N_{5.3<|\eta^{\pm}|_{\min}<6.5}/N_{\mathrm{visible}} = 0.61 \pm 0.15$ and $N_{4.7<|\eta^{\pm}|_{\min}<6.5}/N_{\mathrm{visible}} = 0.89 \pm 0.12$. Since all the $4.7 < |\eta^{\pm}|_{\min} < 5.3$ events are not visible, the correction factor $N_{4.7<|\eta^{\pm}|_{\min}<6.5}/N_{\mathrm{visible}} = 0.89 \pm 0.12$ includes two components: a share of visible events that have $4.7 < |\eta^{\pm}|_{\min} < 6.5(0.80)$ and a correction for events that are not visible by the selection (1.11). The uncertainties of the correction factors were estimated by comparing the nominal correction to the one derived from PHOJET. These correction factors take into account both sides of the IP.

TABLE IV. Summary of statistical and systematic uncertainties ($\mu$b).

| | $I$ | $D11$ | $D22$ | $D12$ | $D21$ |
|---|---|---|---|---|---|
| Statistical | 1.5 | 1.1 | 0.7 | 0.9 | 0.9 |
| Background estimate | 9.0 | 6.0 | 3.5 | 2.7 | 2.2 |
| Trigger efficiency | 2.1 | 1.2 | 1.0 | 0.9 | 0.9 |
| Pileup correction | 2.4 | 2.1 | 0.4 | 1.1 | 1.0 |
| $T1$ multiplicity | 7.0 | 3.9 | 0.7 | 1.6 | 1.7 |
| Luminosity | 4.7 | 2.6 | 0.5 | 1.1 | 1.1 |
| Experimental correction | 14.7 | 14.1 | 2.6 | 2.0 | 2.0 |
| $\eta_{\min}$ | 15.4 | 11.0 | 1.5 | 2.9 | 2.9 |
| Total uncertainty | 24.8 | 19.6 | 4.8 | 5.1 | 4.9 |

Because the choice of $4.7 < |\eta^{\pm}|_{\min} < 6.5$ provides smaller uncertainty, the visible $\eta$ range was extended to $|\eta| = 4.7$ to minimize the model dependence in this final correction. Otherwise, the share of $4.7 < |\eta^{\pm}|_{\min} < 5.3$ events would have been the dominating systematic uncertainty. In this Letter, the $\eta_{\min}$ corrected cross section ($4.7 < |\eta^{\pm}|_{\min} < 6.5$) is called $I$, and the subcategories are $D11$ ($4.7 < |\eta^{\pm}|_{\min} < 5.9$), $D22$ ($5.9 < |\eta^{\pm}|_{\min} < 6.5$), $D12$ ($4.7 < |\eta^{+}|_{\min} < 5.9$ and $5.9 < |\eta^{-}|_{\min} < 6.5$), and $D21$ ($5.9 < |\eta^{+}|_{\min} < 6.5$ and $4.7 < |\eta^{-}|_{\min} < 5.9$).

The sources and values of systematic uncertainties are summarized in Table IV. For each source of systematic uncertainty, the value was calculated by varying the source within its uncertainty and recalculating the measured cross section. The difference between the nominal and recalculated cross section was taken as the systematic uncertainty.

TOTEM determined $\sigma_{\mathrm{DD}} = (116 \pm 25)$ $\mu$b for events that have both diffractive systems with $4.7 < |\eta|_{\min} < 6.5$. The values for the subcategories are summarized in Table III.

In summary, we have measured the DD cross section in an $\eta$ range where it has never been determined before. The TOTEM measurement is $\sigma_{\mathrm{DD}} = (131 \pm 22)$ $\mu$b for events that have at least one particle in both sides of $5.3 < |\eta| < 6.5$ and no particles within $3.1 < |\eta| < 4.7$. The result was deduced with PYTHIA to $\sigma_{\mathrm{DD}} = (116 \pm 25)$ $\mu$b for events that have both diffractive systems with $4.7 < |\eta|_{\min} < 6.5$. The values for the subcategories are summarized in Table III. The determined cross sections are between the PYTHIA and PHOJET predictions for corresponding $\eta_{\min}$ ranges.

We are grateful to the beam optics development team for the design and the successful commissioning of the high $\beta^*$ optics and to the LHC machine coordinators for

scheduling the dedicated fills. This work was supported by the institutions listed in the author affiliations and partially also by NSF (U.S.), the Magnus Ehrnrooth Foundation (Finland), the Waldemar von Frenckell Foundation (Finland), the Academy of Finland, the Finnish Academy of Science and Letters (The Vilho, Yrjö, and Kalle Väisälä Fund), the OTKA Grant No. NK 101438, 73143 (Hungary), and the NKTH-OTKA Grant No. 74458 (Hungary).

[1] M. Ryskin, A. D. Martin, and V. A. Khoze, Eur. Phys. J. C **54**, 199 (2008).
[2] E. Gotsman, E. Levin, U. Maor, and J. S. Miller, Eur. Phys. J. C **57**, 689 (2008).
[3] S. Ostapchenko, Phys. Lett. B **703**, 588 (2011).
[4] V. A. Khoze, F. Krauss, A. D. Martin, M. G. Ryskin, and K. C. Zapp, Eur. Phys. J. C **69**, 85 (2010).
[5] T. Affolder *et al.*, Phys. Rev. Lett. **87**, 141802 (2001).
[6] B. Abelev *et al.*, Eur. Phys. J. C **73**, 2456 (2013).
[7] V. Berardi *et al.* (TOTEM Collaboration), Report No. CERN-LHCC-2004-002, 2004 (unpublished); V. Berardi *et al.* (TOTEM Collaboration), Report No. CERN-LHCC-2004-020, 2004 (unpublished); G. Anelli *et al.* (TOTEM Collaboration), JINST **3**, S08007 (2008).
[8] $\eta = -\ln[\tan(\theta/2)]$, where $\theta$ is the polar angle.
[9] L. Jenkovszky, O. Kuprash, R. Orava, and A. Salii, arXiv:1211.5841.
[10] M. Berretti, Ph.D. thesis, Università di Siena [Report No. CERN-THESIS-2012-23, 2012 (unpublished)].
[11] G. Antchev *et al.* (TOTEM Collaboration), Report No. CERN-PH-EP-2013-173 (unpublished).
[12] V. Avati *et al.*, *Proceedings of 11th ICATPP Conference, Como, Italy, 2009* (World Scientific Publishing, Singapore, 2010).
[13] G. Antchev *et al.* (TOTEM Collaboration), Europhys. Lett. **101**, 21003 (2013).
[14] T. Sjostrand, S. Mrenna, and P. Skands, Comput. Phys. Commun. **178**, 852 (2008).
[15] R. Engel, Z. Phys. C **66**, 203 (1995).
[16] S. Ostapchenko, Nucl. Phys. B, Proc. Suppl. **151**, 143 (2006).

G. Antchev,[1] P. Aspell,[2] I. Atanassov,[2,1] V. Avati,[2] J. Baechler,[2] V. Berardi,[3,4] M. Berretti,[5,6] E. Bossini,[5,6] U. Bottigli,[6] M. Bozzo,[7,8] E. Brücken,[9,10] A. Buzzo,[7] F. S. Cafagna,[3] M. G. Catanesi,[3] C. Covault,[11] M. Csanád,[12,*] T. Csörgő,[12] M. Deile,[2] K. Eggert,[11] V. Eremin,[13] F. Ferro,[7] A. Fiergolski,[14,3] F. Garcia,[9] S. Giani,[2] V. Greco,[6] L. Grzanka,[2,†] J. Heino,[9] T. Hilden,[9,10] A. Karev,[2] J. Kašpar,[15,2] J. Kopal,[15,2] V. Kundrát,[15] K. Kurvinen,[9] S. Lami,[5] G. Latino,[6] R. Lauhakangas,[9] T. Leszko,[14] E. Lippmaa,[16] J. Lippmaa,[16] M. Lokajíček,[15] L. Losurdo,[6] M. Lo Vetere,[7,8] F. Lucas Rodríguez,[2] M. Macrí,[7] T. Mäki,[9,‡] A. Mercadante,[3] N. Minafra,[3,4] S. Minutoli,[2,7] F. Nemes,[12,*] H. Niewiadomski,[6] E. Oliveri,[6] F. Oljemark,[9,10] R. Orava,[9,10] M. Oriunno,[2,§] K. Österberg,[9,10] P. Palazzi,[6] J. Procházka,[15] M. Quinto,[3,4] E. Radermacher,[6] E. Radicioni,[3] F. Ravotti,[2] E. Robutti,[7] L. Ropelewski,[2] G. Ruggiero,[2] H. Saarikko,[9,10] A. Scribano,[6] J. Smajek,[2] W. Snoeys,[2] J. Sziklai,[12] C. Taylor,[11] N. Turini,[6] V. Vacek,[17] M. Vítek,[17] J. Welti,[9,10] J. Whitmore,[18] and P. Wyszkowski[2,‖]

(TOTEM Collaboration)

[1]*INRNE-BAS, Institute for Nuclear Research and Nuclear Energy, Bulgarian Academy of Sciences, 1113 Sofia, Bulgaria*
[2]*CERN, 1211 Geneva, Switzerland*
[3]*INFN Sezione di Bari, 70126 Bari, Italy*
[4]*Dipartimento Interateneo di Fisica di Bari, 70126 Bari, Italy*
[5]*INFN Sezione di Pisa, 56127 Pisa, Italy*
[6]*Università degli Studi di Siena and Gruppo Collegato INFN di Siena, 53100 Siena, Italy*
[7]*INFN Sezione di Genova, 16146 Genova, Italy*
[8]*Università degli Studi di Genova, 16146 Genova, Italy*
[9]*Helsinki Institute of Physics, 00014 Helsinki, Finland*
[10]*Department of Physics, University of Helsinki, 00014 Helsinki, Finland*
[11]*Case Western Reserve University, Department of Physics, Cleveland, Ohio 44106, USA*
[12]*MTA Wigner Research Center, RMKI, 1525 Budapest, Hungary*
[13]*Ioffe Physical-Technical Institute of Russian Academy of Sciences, 194021 St. Petersburg, Russian Federation*
[14]*Warsaw University of Technology, 00662 Warsaw, Poland*
[15]*Institute of Physics of the Academy of Sciences of the Czech Republic, 18221 Praha, Czech Republic*
[16]*National Institute of Chemical Physics and Biophysics NICPB, 12618 Tallinn, Estonia*
[17]*Czech Technical University, 11519 Praha, Czech Republic*
[18]*Penn State University, Department of Physics, University Park, Pennsylvania 16802, USA*

[*]Also at Department of Atomic Physics, Eötvös University, 1117 Budapest, Hungary.
[†]Also at Institute of Nuclear Physics, Polish Academy of Science, 31342 Krakow, Poland.
[‡]Corresponding author.
tuula.maki@cern.ch
[§]Also at SLAC National Accelerator Laboratory, Stanford, CA 94025, USA.
[‖]Also at AGH University of Science and Technology, 94025 Krakow, Poland.